ELSEVIER

International Journal of Fatigue 23 (2001) 619–626

International Journal of Fatigue

www.elsevier.com/locate/ijfatigue

Influence of nickel on the susceptibility to corrosion fatigue of duplex stainless steel welds

S.A. Távara [a], M.D. Chapetti [b,*], J.L. Otegui [b], C. Manfredi [b]

[a] *Department of Physics, University Trujillo, Peru*
[b] *INTEMA, University of Mar del Plata, J.B. Justo 4302, 7600 Mar del Plata, Argentina*

Received 22 September 1999; received in revised form 22 October 2000; accepted 7 January 2001

Abstract

The object of this work is to analyse the mechanisms of corrosion fatigue and to study the influence of Nickel on the susceptibility to corrosion fatigue in welded Duplex stainless steels. A 'Ferralium 255' type cast Duplex stainless steel was used as base material. Four types of experimental electrodes of chemical composition similar to base material were used, with varying compositions of Ni (2.8, 4.7, 6.8 and 9.8 wt%). Experimental three point bending fatigue tests were carried out in air at 10 Hz, and in normalised seawater at 3 Hz, with anodic polarisation to 800 mV ECS. The strain gauge technique was used to monitor subcritical propagation of cracks. The effect of the corrosive environment on crack growth rates and on the coefficients of the Paris equation were assessed for each type of electrode. Comparing the experimental results, it was determined that the best electrode is the one that contains 4.7% Ni.

Keywords: Corrosion fatigue; Stainless steel; Weld metal

1. Introduction

The Duplex stainless steels are iron based alloys that possess a two phase microstructure: austenite and delta ferrite in approximately similar percentages. They have an excellent combination of such properties as greater yield strength than austenitic stainless steels, resistance to general corrosion, resistance to intergranular corrosion, resistance to pit and crevice corrosion, resistance to stress corrosion cracking, appropriate weldability [1]. The Duplex stainless steels have become important competitors to the austenitic stainless steels in many applications, and attention has been located in the aspects of welding. The introduction of modern grades with better properties and a competitive price have increased their use, for example in offshore industries, petrochemical plants and naval constructions. An important limitation of the Duplex stainless steel is its maximum temperature of service, below 300°C, due to the problem of brittleness at 475°C [2–4].

Duplex steels are susceptible to chloride-induced SCC and corrosion fatigue but they clearly offer useful benefits over austenitic grades in terms of cracking resistance [5]. The advantage of the Duplex alloys in media that contain chloride resides in the content of delta ferrite, which promotes combined effects due to electrochemical and mechanical factors. Owing to different elastic limits, which are lower in austenite than in ferrite, plastic deformation under an external load concentrates on the austenite, while ferrite acts as an anode protecting the austenite that acts as a cathode [6].

It is normal practice in fusion welding to match the composition of the filler material of the base metal as far as possible, so corrosion and mechanical properties equivalent to those of the parent material can be obtained. With Duplex stainless steel the situation is different since matching composition consumables will result in an appreciably higher ferrite content in the weld than in the parent metal.

Segregation of alloying elements is inevitable in welding ferritic/austenitic steels, not only in weld metal during solidification, but also in the HAZ. The effects of

* Corresponding author. Tel.: +54-23-81-6600; fax: +54-23-81-0046.
E-mail address: intema@fi.mdp.edu.ar (M.D. Chapetti).

0142-1123/01/$ - see front matter
PII: S0142-1123(01)00018-4

Table 1
Chemical compositions and ferrite content

Element	Base material	Elect 'A'	Elect 'B'	Elect 'C'	Elect 'D'
Ni	4.8	2.8	4.7	6.83	8.90
Cr	25.60	23.5	23.8	23.3	23.20
C	0.06	0.03	0.03	0.03	0.03
Mo	3.18	2.56	2.57	2.57	2.54
Mn	0.73	0.74	0.8	0.81	0.81
Si	1.0	0.6	0.62	0.65	0.64
O	0.097	0.096	0.097	0.086	0.087
N	0.022	0.021	0.021	0.021	0.022
P	0.027	0.017	0.011	0.016	0.017
S	0.006	0.005	0.005	0.006	0.006
% ferrite	54.6	55.2	50.3	34.7	21.8

Table 2
Mechanical properties

Prop.	Base material	Elect 'A'	Elect 'B'	Elect 'C'	Elect 'D'
σ_y (MPa)	570	576	625	652	612
σ_{UTS} (MPa)	750	765	829	853	817

Table 3
Charpy properties

Test temp.	Base material	Elect 'A'	Elect 'B'	Elect 'C'	Elect 'D'
−20°C	8	4	17	36	35
0	10	5	30	42	39
+20°C	12	6	36	48	44

alloying elements on general and pitting corrosion resistance of Duplex stainless steels have been studied previously. Results indicate that corrosion resistance of welded parts made of these alloys are less resistant than base metal because of the oxide layer formed during the welding process. Control of carbon content (low carbon), alloy balance and welding conditions to ensure austenite formation can make corrosion resistance of duplex weldments equivalent to that of the base metal in most service environments [7].

Balance of the austenite/ferrite contents of welded Duplex stainless steels is dependent upon electrode composition. Ni plays an important role in this balance as austenite promoter. Ni content also adds to pitting resistance. Optimum Ni should be maintained within a narrow range of 4–7% for 22% Cr alloys and 4–8% for 25% Cr alloys in order to obtain optimum pitting resistance [8].

Owing to the heterogeneity of the welded materials, they are more susceptible to attack by localised corrosion, particularly in media containing aggressive ions. Corrosion fatigue in welded joints is considered a very dangerous type of propagation of defects in materials that are subjected to dynamic loads in a corrosive medium [9]. It describes in-service subcritical growth of cracks induced by the simultaneous interaction of mechanical, metallurgical and electrochemical factors. The interdependent variables that can affect the initiation and propagation of such cracks are: magnitude and frequency of cyclic stress; residual stresses; mean stress; corrosive medium; electrochemical potential; concentrations of aggressive ions; temperature; microstructure; alloy chemical composition; number, type, shape and size of non metallic inclusions; type, shape, size and distribution of typical initial defects due to the welding process; severity of these defects as initiators (this is, if they are really plane or there will be an important period of crack initiation); shape and direction in which the formed cracks grow; segregation of alloy elements, etc. [10].

For the fracture mechanics characterisation of a material under conditions of cyclic load in an aggressive medium, the methods of linear elastic fracture mechanics (LEFM) associate the applied amplitude of the cyclic crack tip stress intensity factor (ΔK) with the crack propagation rate in the material (da/dN). The experi-

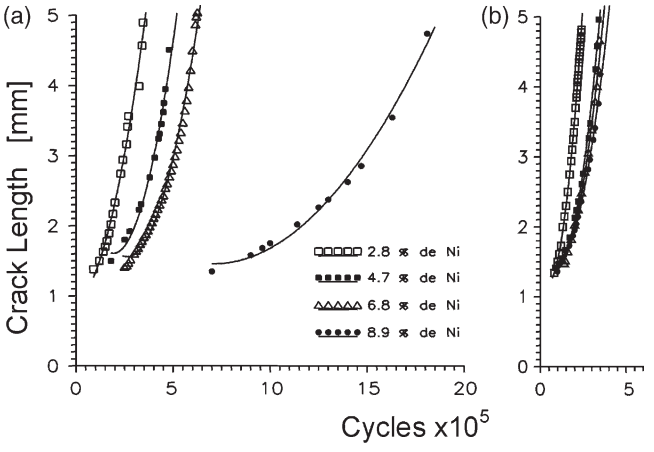

Fig. 1. Crack depths a as a function of the number of cycles in air (a) and in seawater (b).

mental equation of Paris and Erdogan is a simple model that assumes an exponential relationship between da/dN and ΔK:

$$\frac{da}{dN}=C(\Delta K)^m \tag{1}$$

where C and m are constants that depend on the material, test conditions and corrosive medium. The environmental contribution to the crack growth rate is:

$$(da/dN)_{cf}=(da/dN)_e-(da/dN)_r \tag{2}$$

where $(da/dN)_e$ is the measured crack growth rate and $(da/dN)_r$ is the reference crack growth rate, corresponding to pure mechanical fatigue in air.

2. Experimental procedure

The purpose of this work is to evaluate the influence of Ni as an alloy element in experimental electrodes for welding Duplex stainless steels, on their corrosion fatigue properties in seawater. The base material used in this investigation is a Duplex stainless steel with an austenite–ferrite microstructure in an as-cast condition (of the type Ferralium 255). Its chemical composition is shown in Table 1, where it can be observed that it presents an inbalance of ferrite-former and austenite-former elements. Since the best properties of Duplex stainless steel are achieved when the percentages of both phases are approximately the same, a thermal treatment was made to 1050°C for 1 h, followed by water-cooling. Colour metallography was used to identify the phases [11]. Metallography was made by using grids of 546 points at 200× magnification. Austenite content was calculated by counting the points that fall inside the austenite islands. The mechanical properties of the resulting base material after heat treatment are shown in Tables 2 and 3.

Four types of 3.25-mm-diameter SMAW electrodes were analysed. Chemical composition was in all cases similar to base metal (Table 1), except Ni content. Nickel compositions were 2.8, 4.7, 6.8 and 8.9% for deposited metals with electrodes A, B, C and D, respectively. Ferrite content was measured on all weld metal samples using magnetic methods. Their mechanical properties are shown in Table 2. Charpy tests were made at −20, 0 and 20°C and the results are shown in Table 3.

Multipass manual welds were made, keeping heat imputs at about 1.5 kJ and minimum interpass temperatures over 150°C.

Welded specimens were machined and eight three-point bending specimens were obtained (two specimens for each electrode). In order to concentrate the initiation of the crack in a specific place, a shallow semielliptical defect (about 0.5–1 mm deep) was introduced in the specimens using an electro discharge technique. Three-point bending fatigue tests were carried out in a load-control walking-beam fatigue machine, using a minimum-to-maximum load ratio R=0.2. Specimens were tested in air to a frequency of 10 Hz, and in artificial normalised seawater to a frequency of 3 Hz. Applied loads were 20 000 N and an electrochemical potential of +800 mV ECS was constantly kept in order to evaluate the effect of the corrosive medium. The pH of the solution was controlled and maintained during the test at a

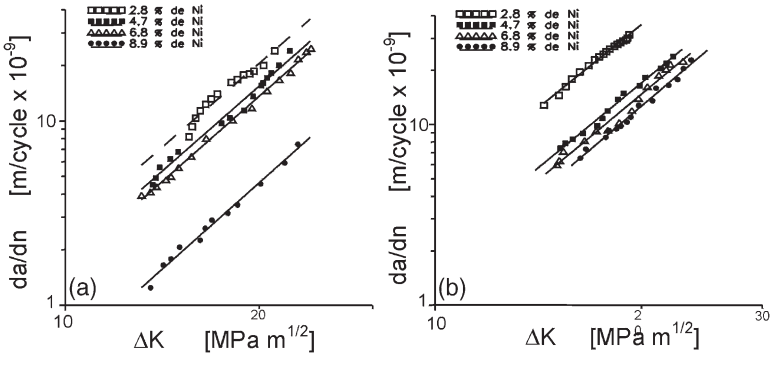

Fig. 2. Crack growth rates in air (a) and in seawater (b).

Table 4
Paris constants in air and seawater

Fatigue parameters	Elect 'A' 2.80 (%) Ni	Elect 'B' 4.70 (%) Ni	Elect 'C' 6.83 (%) Ni	Elect 'D' 8.90 (%) Ni
In air				
C ($\times 10^{-12}$ m/ciclos)	2.41	1.59	1.36	0.41
m	3.02	3.06	3.07	3.11
In normalised seawater, 800 mV ECS, f=3 Hz				
C ($\times 10^{-12}$ m/ciclos)	3.76	1.47	1.36	0.81
m	3.05	3.12	3.16	3.21

Table 5
Fatigue crack growth lives (N_P) spent growing the crack from a depth of 1.5 mm to 5 mm

N_P	Elect 'A'	Elect 'B'	Elect 'C'	Elect 'D'
Seawater	165 000	250 000	270 000	300 000
Air	250 000	350 000	410 000	1 050 000

value of 8.2. Refill of corrosive medium was made every 8 h. The tests were carried out at room temperature.

Multiple strain gauges were applied near the defect to detect variations in compliance arising from crack initiation and early growth. One strip containing ten 2.1-mm-long strain gauges was bonded to the plate surface, about 3 mm from the defect. Details of this monitoring technique are given elsewhere [12]. Only a few beach or ink marks were necessary to fit a calibration curve for each strain gauge, decreasing the error in the measurement of crack depth to about 5%. Errors in the measurement of compliance due to system variations were estimated at about 0.5%. When determining crack propagation rates, errors are minimised owing to the substraction of two consecutive readings of the same variable (crack depth), because measurement error consistently occurs in only one direction.

'Post mortem' indications of the crack development were made by ink marking, in fatigue tests in air, and by beach marking by a 50% reduction of the cyclic load in fatigue tests in normalised seawater. Fractographic observations were made on SEM at magnifications up to 10 000×. Prior to observation, the specimens were cleaned in 5% HCl+acidic inhibitor to remove corrosion products and then dipped in acetone and hot air dried. Finally, experimentally determined da/dN and ΔK values were plotted on logarithmic graphs to obtain the experimental values of Paris C and m constants, see Figs. 1 and 2. The calculated Paris coefficients in the analysed region are shown in Table 4 for each case. Table 5 shows the fatigue crack growth lives spent to grow the crack from a depth of 1.5 mm to 5 mm (see also Fig. 1).

Polarisation curves in artificial seawater for each electrode were made by stepwise polarisation at a rate of 4 mV/min. Results of these tests are shown in Fig. 3. Pitting corrosion potential as function of Ni content of the electrode is shown in Table 6.

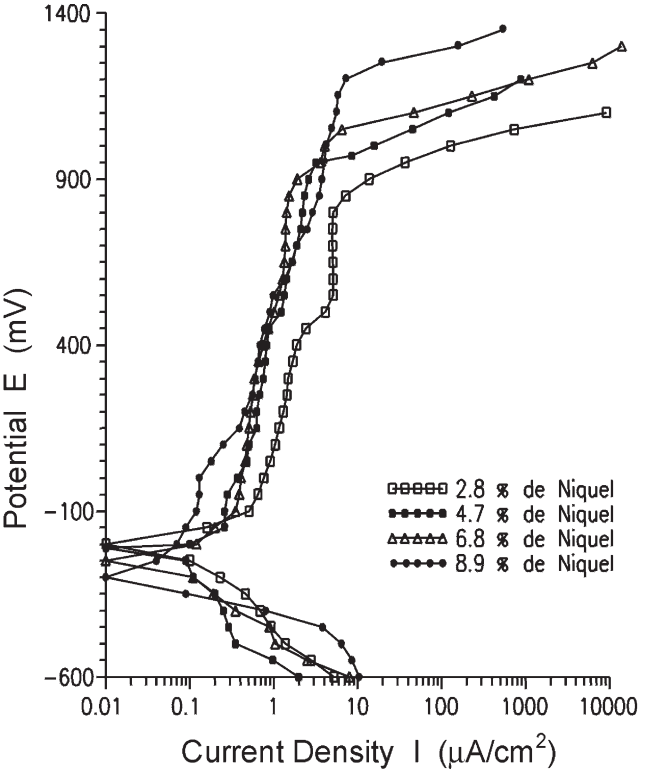

Fig. 3. Polarisation curves in artificial seawater.

Table 6
Corrosion and pitting potentials obtained from the polarisation curves

Electrochemical variables	Elect 'A' 2.80 (%) Ni	Elect 'B' 4.70 (%) Ni	Elect 'C' 6.83 (%) Ni	Elect 'D' 8.90 (%) Ni
E_{CORR} (mV)	−202	−212	−245	−280
$E_{PITTING}$ (mV)	900	970	1050	1140

3. Discussion

Anodic polarisation curves (Fig. 3) show that all the electrodes exhibited a similar passive behaviour with current densities in the passive region decreasing as the Ni content increased. The decrease in current density is more evident between the 2.8% Ni electrode and the other electrodes. Pitting corrosion potential increases with Ni content, with a maximum value of 1140 mV_{SCE} for the 8.9% Ni electrode (Table 6). Corrosion potential also shows a tendency to more negative values as the Ni content of the weld metal increases. As a consequence of both effects (increase of pitting potential and decrease of corrosion potential), the passive region increases with Ni content. These beneficial effects of Ni can be produced by an enrichment of Ni in the passive film.

Fig. 1(a) shows crack depths as a function of the number of fatigue cycles in air, from an 'initiation' size of 1.5 mm up to a final depth of about 5 mm. The value of 1.5 mm was selected as an initial size for processing fatigue data because post mortem analyses of the fractured specimens show consistently that for that depth the cracks are already well developed from the machined notches, and already have a semi-elliptical shape. This allows us to apply a simple equation to evaluate the applied ΔK in a normal fracture mechanics analysis, using the Newman–Raju equations [13].

The effect of Ni content on the number of cycles for fatigue initiation is clear. Ni content has a direct relation to the number of cycles necessary to reach a depth of 1.5 mm, from approximately 100 000 cycles for the 2.8% Ni electrode up to 600 000 cycles to the 8.9% Ni electrode. In the case of fatigue in air, it is known that the influence of Ni comes from the fact that increasing Ni content improves both strength and toughness. This is verified by Tables 2 and 3. These tables show that tensile and impact properties are also affected by nickel content. In this case the electrode with 6.8% Ni presents the best combination of properties. Fig. 1(b) shows crack depths as a function of the number of fatigue cycles in artificial seawater. Note the increase in growth rates and the decrease in fatigue initiation times. In this case there is no clear effect of Ni content on the number of cycles for initiation, probably because the accelerating effect of the corrosive medium makes any possible effect of Ni secondary.

Fig. 2 shows crack propagation rates as a function of the stress intensity factor range ΔK, in air and in seawater, for the four electrodes tested. These curves were obtained from the *a–N* data shown in Fig. 1. The marked influence of the corrosive medium is clearly observed. Crack propagation rates in air show a clear difference between the 8.9% Ni electrode and the others. These lowest crack propagation rates can be related to the high content of the austenitic phase in the metal deposited by these electrodes. Fractographs of test samples in air show a clear relation of the fracture mode with Ni content. There is a tendency from quasi-cleavage fracture for the 2.8% Ni electrode, as shown in Figs. 4(a) and (b), up to 100% ductile tearing (as shown in Fig. 5), as nickel content increases.

This is directly related to the differences in microstructural composition. Crack propagation in austenite phases occurs by a mechanism of coalescence of

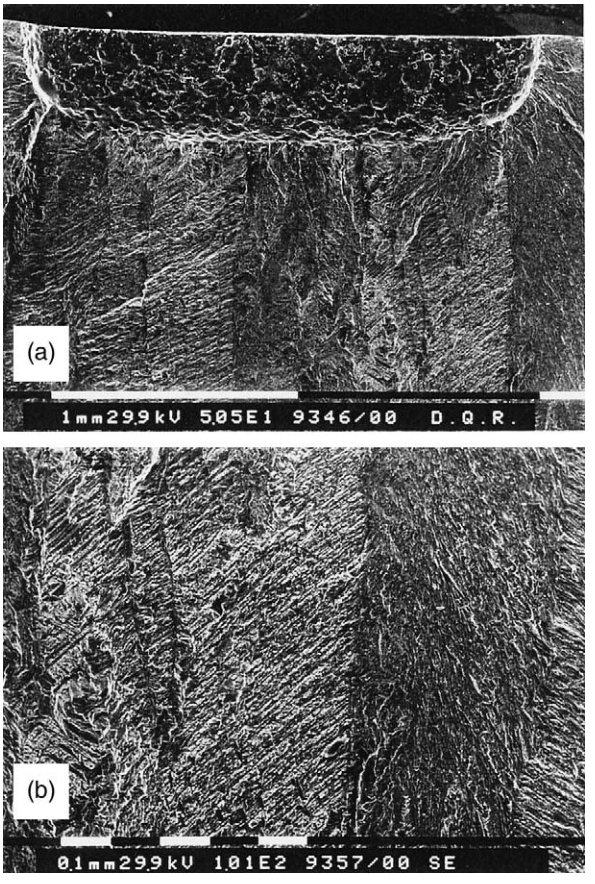

Fig. 4. Fractographs of 2.8% Ni samples tested in air.

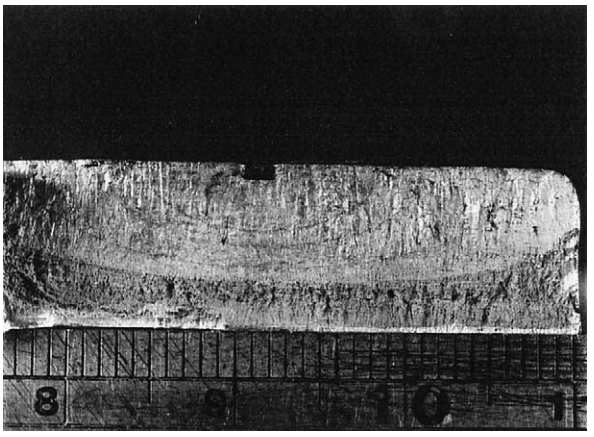

Fig. 5. Fractographs of 6.8% Ni samples tested in air.

microvoids, while for the ferrite phase crack propagation is for the most part due to cleavage (see Fig. 6). The largest difference occurs when austenite increases from about 65% (electrode C) to about 78% (electrode D).

Test results of corrosion fatigue in artificial seawater to an anodic potential of +800 mV ECS show an influence of Ni which is different from the trend observed in the fatigue tests in air. Only test results for the weld metal with 2.8% Ni differ markedly, while the three remaining compositions show a minimum difference regarding crack propagation rates. The 2.8% Ni electrode shows a tendency to intergranular and quasi-cleavage fracture (Fig. 6), again due to its microstructure having a high ferrite content. The rest of the welds show transgranular fracture and evidence anodic dissolution of the crack surface (Fig. 7). Depending on the Ni content, anodic dissolution is observed either located in non-metallic inclusions, such as manganese sulphide, or as a phase that has been totally dissolved, where only remaining products of corrosion are observed. In this case the largest difference occurs when austenite increases from about 45% (electrode A) to about 50% (electrode B). It can be argued, therefore, that smaller percentages of Ni can mean a larger improvement in the fatigue life of these welds, when tested in seawater.

The C and m coefficients of the Paris equation (Eq. (1)) were calculated from the graphs of Fig. 2, for each electrode in each medium. Table 4 shows that a small increase in the Paris exponent m is observed as Ni content increases. It can be inferred that Ni content increases the effective values of ΔK for deeper cracks. The relationship between da/dN and ΔK depends not only on the material intrinsic growth parameters, but also on

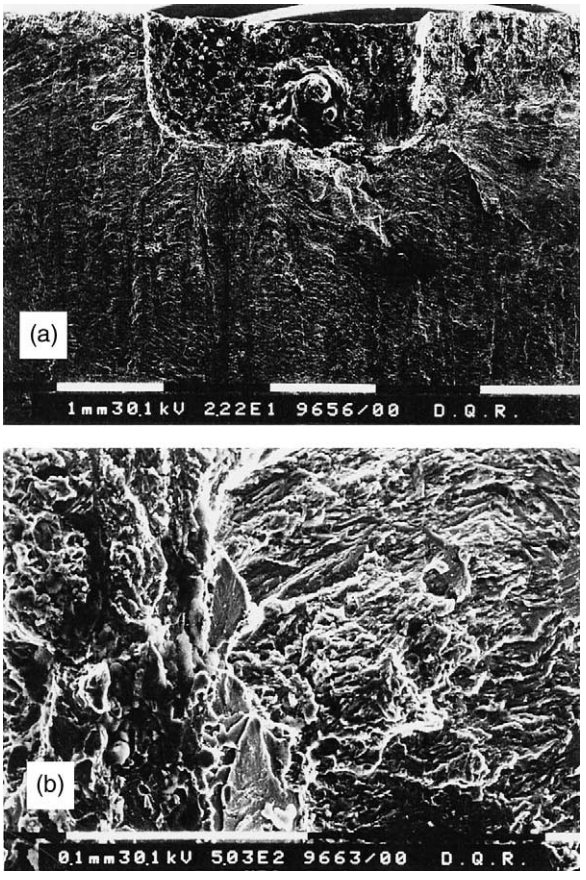

Fig. 6. Fractographs of 2.8% Ni samples tested in seawater.

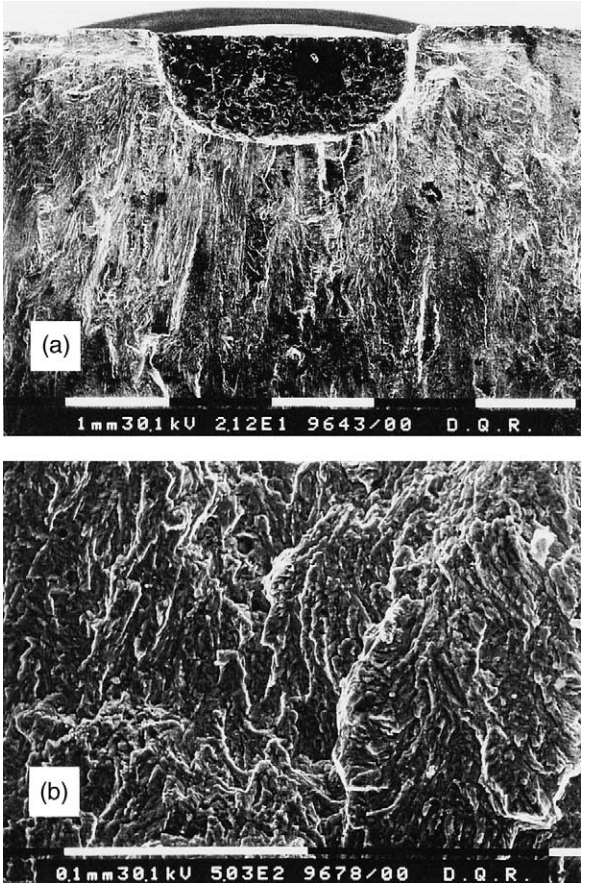

Fig. 7. Fractographs of samples tested in seawater: (a) 8.9% Ni; (b) 6.8% Ni.

Table 7
Crack propagation rates

Electrode	$(da/dN)_r$ (m/cycle×10^{-9})	$(da/dN)_{cf}$ (m/cycle×10^{-9})	$(da/dN)_e$ (m/cycle×10^{-9})	Contribution corrosion electrolyte (%)
2.8% Ni	58	80	22	37.9
4.7% Ni	24	35	11	45.8
6.8% Ni	15	25	10	66.7
8.9% Ni	5	19	14	280.0

extrinsic factors depending on the actual load, specimen and crack growth conditions. Table 4 also shows a marked decrease of the constant C with Ni content, this directly related to the beneficial effect of Ni on fatigue crack propagation rates in both air and seawater. Not so clear is the expected trend to larger C values in the case of tests in seawater, indicating faster crack growth. Notable exceptions are electrodes B and C. The small increase in fatigue crack propagation rates observed in Fig. 2 when comparing air and seawater media are completely absorbed in these two cases by a slight increase in the Paris exponent m. In other words, the increase in crack growth rates occurs mainly when the cracks are deeper.

The contribution of the corrosion electrolyte to crack propagation rates was calculated from Eq. (2). The values obtained can be seen for a crack length of 4.5 mm in Table 7. The results indicate a factor of 2 between the largest and smallest contributions of the corrosive medium to fatigue growth rates (values from 22 m/cycle×10^{-9} to 10 m/cycle×10^{-9}). The relative contribution of the corrosive electrolyte to crack rates increases as Ni content increases, from 38% to 280%. This effect is related to the one order of magnitude decrease of crack growth rates in air as the Ni content increases.

Making an overall comparison of mechanical, fatigue and corrosion properties of the welded joints tested, it is concluded that the optimum amount of Ni is around 4.7%. Although joints made with 8.9% Ni electrodes show better properties with regard to localised corrosion attack (pitting potential) and fatigue in air, the improvement regarding corrosion-fatigue behaviour with 6.8% and 8.9% Ni electrodes is minimum. Taking into account the high price of Ni and the expected operative life of components subjected to corrosion fatigue, the 4.7% Ni electrode is considered the most suitable option. When looking at the 'air' data and the results, the 8.9% Ni electrode is clearly the best.

4. Conclusions

Experimental three-point bending corrosion fatigue tests were carried out in normalised seawater on welded Duplex stainless steels with four experimental electrodes varying in Ni content. The strain gauge technique was used to monitor subcritical propagation of cracks. The effects of the corrosive environment on crack growth rates and on the coefficients of the Paris equation were assessed for each type of electrode.

Regarding mechanical properties of the weld joints, it is concluded that the optimum amount of Ni is around 4.7%. Although joints made with 8.9% Ni electrodes showed better properties with regard to localised corrosion attack (pitting potential) and fatigue in air, the improvement regarding corrosion-fatigue behaviour is minimum. Taking into account the high price of Ni and the expected operative life of components subjected to corrosion fatigue, the 4.7% Ni electrode is considered the most suitable option.

Acknowledgements

The authors acknowledge financial support from the International Program in Physical Sciences (IPPS-Sweden) and the Consejo Nacional de Investigaciones Cientificas de la Republica Argentina (CONICET). Thanks are also extended to Dr. Estela Surian for technical advice, and to CONARCO SA, Argentina, for help in manufacturing experimental electrodes.

References

[1] Folkhard E. Welding Metallurgy of Stainless Steels. Wien/New York: Springer Verlag, 1988.
[2] Nilsson JO. Super Duplex stainless steels. Mater Sci Technol 1992;8:685–700.
[3] Baeslack WA, Lippold JC. Phase transformation behaviour in Duplex stainless steel weldments. Metal Construct 1988;January.
[4] Lundqvist B, Norberg P. Weldability aspects and weld joint propierties of Duplex stainless steels. Welding J 1988;77(5):45–51.
[5] Carlen JC. Werkstoffe Korrosion 1970;21:645–50.
[6] Magnin y Col T. Coupling effects between the a and g phases during corrosion fatigue of an a/g Duplex stainless steel. In: Fatigue '87, Third International Conference on Fatigue and Fatigue Thresholds, vol. III, 1987:1221.
[7] Peterson WA, Lang FW. Weld J, 1970;49:267s.
[8] Richardson WH, Gupa P. Br Corr J 1979;14:167.

[9] S. Lambert, Fatigue crack growth welded joints in seawater. Ph.D Thesis, Faculty of Engineering, University of Waterloo, Canada, 1988.
[10] Krausz K. The Development of the Constitutive Law of Crack Growth in Corrosion Fatigue. In: Handbook of Fatigue Crack Propagation in Metallic Structures, 3.1.3, 1994.
[11] Thier y Col. Color metallography. Metal Construct 1987;March.
[12] Otegui JL, Mohaupth UH, Burns DJ. A strain gauge technique for monitoring small fatigue crack in welds. Eng Fract Mech 1991;40(3):549–70.
[13] Newman JC, Raju IS. An empirical stress intensity factor equation for the surface crack. Eng Fract Mech 1981;15(1-2):185–92.